2.0×10^{-9} cm^{-2} sr^{-1} sec^{-1} at a 90% confidence level. While this is not in disagreement with our previous result[1] of $(2.1_{-1.5}^{+1.8})\times10^{-9}$ cm^{-2} sr^{-1} sec^{-1}, any residual positive indication of the existence of quarks is effectively eliminated.

Recent results by Buhler-Broglin *et al.*[2] and by Lamb *et al.*[3] are also negative at similar significance levels.

The cross section for the production of quarks in nucleon-nucleon interactions deduced from the measured flux is somewhat model-dependent. It is convenient to consider the cross sections for a canonical model defined such that the cross section is constant above threshold. For this model, the flux limit establishes a production cross section limit of about 0.2 μb, for 10-BeV/c^2 quarks, and a limit of about 0.04 μb for a quark mass of 5 BeV/c^2.

[2] A. Buhler-Broglin, G. Fortunato, T. Massam, Th. Muller, and A. Zichichi, in Proceedings of the 13th International Conference on High-Energy Physics, University of California, Berkeley, California, 1966 (unpublished).

[3] R. C. Lamb, R. A. Lundy, T. B. Novey, and D. D. Yovanovitch, in Proceedings of the 13th International Conference on High-Energy Physics, University of California, Berkeley, California, 1966 (unpublished).

PHYSICAL REVIEW VOLUME 154, NUMBER 5 25 FEBRUARY 1967

Double Pion Production without Annihilation in Antiproton-Proton Interactions at 2.7 BeV/c†

H. B. CRAWLEY,* R. A. LEACOCK, and W. J. KERNAN
Institute for Atomic Research and Department of Physics, Iowa State University, Ames, Iowa

(Received 29 August 1966)

A study was made of the reaction $\bar{p}p\to\bar{p}p\pi^+\pi^-$ at 2.7 BeV/c. The total cross section for this reaction was determined to be 1.93±0.16 mb. The data were found to be consistent with 100% $N^*\bar{N}^*$ formation, where N^* is the 1238-MeV pion-nucleon resonance with $T=T_Z=J=\frac{3}{2}$. It was observed that the N^* production is highly peripheral; specifically, 50% of the $\bar{N}^*$'s are formed with $\cos\theta_p>0.8$, where θ_p is the angle between the outgoing $\bar{N}^*$ and incoming $\bar{p}$ momenta in the over-all center-of-mass system. A comparison of the data with predictions of the form-factor and absorption one-pion-exchange models was made.

I. INTRODUCTION

DOUBLE pion production without annihilation in antiproton-proton interactions has been studied at 3.28 and 3.66,[1] 3.6,[2] 5.7,[3,4] and at 6.94 BeV/c.[5] Presented here is an investigation of the reaction

$$\bar{p}+p\to\bar{p}+p+\pi^+\pi^- \qquad (1)$$

at 2.7 BeV/c. The experiment was performed at Brookhaven National Laboratory using the 20-in. hydrogen bubble chamber at the AGS. Preliminary studies of other final states in this experiment are reported elsewhere.[6]

Recently, extensive use has been made of one-meson-exchange models[7] to calculate total cross sections, angular distributions, invariant mass distributions, and decay angular correlations for meson production in meson-nucleon and nucleon-nucleon interactions in the BeV range. These calculations are usually applied to reactions with three- and four-particle final states where the final state can be interpreted as containing one or two resonances. Two of the one-meson-exchange models are the form-factor model of Ferrari and Selleri,[8] and the absorption model, the present form of which is

† This research is based in part on a Ph.D. thesis submitted by H. B. Crawley to Iowa State University, Ames, Iowa. The work was performed in part at the Ames Laboratory of the U. S. Atomic Energy Commission and in part at Brookhaven National Laboratory, Upton, L. I., New York. Contribution No. 1948.

* National Aeronautics and Space Administration Predoctoral Fellow. Present address: Department of Physics, University of Illinois, Urbana, Illinois.

[1] T. Ferbel, A. Firestone, J. Sandweiss, H. D. Taft, M. Gailloud, T. W. Morris, W. J. Willis, A. H. Bachman, P. Baumel, and R. M. Lea, Phys. Rev. **138**, B1528 (1965); T. Ferbel, J. Sandweiss, H. D. Taft, M. Gailloud, T. E. Kalogeropoulos, T. W. Morris, and R. M. Lea, Phys. Rev. Letters **9**, 351 (1962).

[2] H. C. Dehne, E. Lohrmann, E. Raubold, P. Söding, M. W. Teucher, and G. Wolf, Phys. Rev. **136**, B843 (1964).

[3] K. Böckmann, B. Nellen, E. Paul, B. Wagini, I. Borecka, J. Díaz, U. Heeren, U. Liebermeister, E. Lohrmann, E. Raubold, P. Söding, S. S. Wolff, J. Kidd, L. Mandelli, L. Mosca, V. Pelosi, S. Ratti, and L. Tallone, Nuovo Cimento **42**, 954 (1966).

[4] V. Alles-Borelli, B. French, Å. Frisk, and L. Michedja, CERN Report No. CERN/TC/PHYSICS 66-10, 1966 (unpublished).

[5] T. Ferbel, A. Firestone, J. Johnson, J. Sandweiss, and H. D. Taft, Nuovo Cimento **38**, 19 (1965).

[6] W. J. Kernan, D. E. Lyon, and H. B. Crawley, Phys. Rev. Letters **15**, 803 (1965); D. E. Bohning and W. J. Kernan, Bull. Am. Phys. Soc. **10**, 1115 (1965); L. S. Schroeder, D. E. Bohning, W. J. Kernan, V. Domingo, Å. Eide, G. Fisher, R. Sears, and J. Von Krogh, *ibid.* **11**, 360 (1966); W. J. Kernan, D. E. Bohning, L. S. Schroeder, V. Domingo, Å. Eide, G. Fisher, R. Sears, and J. Von Krogh, *ibid.* **11**, 360 (1966).

[7] In the present paper no attempt is made to provide complete references to the literature on one-meson-exchange models. For an extensive review of the development and present status of these models (also called peripheral models) see A. C. Hearn and S. D. Drell, Stanford University Report No. SLAC-PUB-176, 1966 (unpublished).

[8] E. Ferrari and F. Selleri, Nuovo Cimento Suppl. **24**, 453 (1962).

due to Sopkovich,[9] Durand and Chiu,[10] and Gottfried and Jackson.[11,12] The relative merits of the two approaches have been discussed in the literature.[12,13] The experimental results reported in the present paper are compared with the predictions of both models.

The experimental techniques are outlined in Sec. II, while the main experimental results are presented in Sec. III. The data are compared with the predictions of the form-factor and absorption models in Sec. IV, and the main results of the present and previous experiments are summarized in Sec. V.

II. EXPERIMENTAL PROCEDURE

The Brookhaven National Laboratory 20-in. hydrogen bubble chamber was exposed to a beam of 2.7-BeV/c antiprotons in the Yale-BNL[14] separated beam, in a collaborative experiment by groups from Iowa State University and the University of Colorado. A total of 91 000 pictures was taken.

The beam contamination was studied in a number of ways. All the methods, including an analysis of the energy distribution of δ rays from the beam tracks, yield consistent answers that the beam is more than 99% antiprotons.

The beam flux was determined by counting the beam tracks entering the fiducial volume on every tenth frame of a sample of the film. The beam flux was found to be 11.9 beam tracks per frame.

The analysis of all strange-particle reactions is being carried out in collaboration by the two groups. For the reactions not involving strange particles the University of Colorado is analyzing the two-prong events, and Iowa State University is analyzing the four- and six-prong events. The four-prong events which were used for the study of reaction (1) were taken from a sample of 45 000 frames. All frames were scanned twice, and all differences in the scans were checked to determine the correct assignment. These scans were, respectively, 94.7 and 97.0% efficient for correct identification of four-prong events. All four-prong events in a restricted fiducial region were measured in approximately 18 000 pictures. These events were measured in three views, reconstructed in space, and kinematically fitted using the program GUTS.[15] An attempt was made to fit each event to all mass hypotheses for four or five particles in the final state consistent with the selection rules of the strong interactions. The following conditions were used:

(1) For four-constraint cases (no missing neutral particles) the missing mass was required to be within three standard deviations of zero.

(2) For one-constraint cases (one missing neutral particle) the missing mass had to be consistent with the mass of the assumed neutral particle within three standard deviations.

(3) The χ^2 cutoff for four-constraint cases was $\chi^2 \leq 15$.

(4) The χ^2 cutoff for one-constraint cases was $\chi^2 \leq 9$.

All events that had a fit to reaction (1) were then ionization checked for consistency. In this first sample of 18 000 frames approximately 95% of the events which had one or more four-constraint fits to reaction (1) satisfied the ionization check. These events were then used to establish scanning criteria under which a special sample of four-prong events was selected from the remainder of the film for measuring in the study of this reaction. These criteria were chosen to ensure selection of all events of type (1), while still reducing the measuring by a factor of 6.

After all such selected events found in a somewhat larger fiducial volume in 43 500 good quality pictures had been measured, a check of the selection procedure was carried out. This was accomplished by measuring all four-prong events in the same increased fiducial volume in 4500 pictures not included in the first sample of 18 000 pictures and checking that all acceptable fits to reaction (1) in this second sample had been found in the special measuring procedure.

After further studies, the acceptance criteria for four-constraint fits to reaction (1) were relaxed. In particular, the χ^2 cutoff was increased to ≤ 31, and the missing-mass test was increased to five standard deviations. In this reaction, the rigid ionization criterion keeps the relaxed acceptance criteria from introducing a significant background.

The final sample consists of 719 events accepted as being due to reaction (1). Losses from all sources, nonmeasurable events, scan losses, etc. are estimated to account for another 80 events.

A possible background reaction which could yield accidental fits to reaction (1) while passing the ionization test is the process

$$\bar{p}+p \rightarrow \bar{p}+p+\pi^+ +\pi^- +\pi^0. \qquad (2)$$

Despite the relaxed criteria of five standard deviations on missing-mass tests, χ^2 cutoffs of ≤ 31 for four-constraint fits and ≤ 13 for one-constraint fits, no event has an ionization consistent fit to both reactions (1) and (2). Hence the sample of 719 events contains no events with consistent fits to both reactions (1) and (2). This is due, at least in part, to the cross section for reaction (2), which is down by a factor of 20 from that for reaction (1).

The possibility of biases in the data was examined by looking for apparent violations of C or CP invariance in all of the distributions examined which are subject

[9] N. J. Sopkovich, thesis, Carnegie Institute of Technology, 1962 (unpublished); Nuovo Cimento **26**, 186 (1962).

[10] L. Durand, III, and Y. T. Chiu, Phys. Rev. **139**, B646 (1965), and references therein.

[11] K. Gottfried and J. D. Jackson, Nuovo Cimento **34**, 735 (1964).

[12] J. D. Jackson, Rev. Mod. Phys. **37**, 484 (1965). This article is a comprehensive review of the absorption model.

[13] F. Selleri, Nuovo Cimento **42**, 835 (1966).

[14] C. Baltay, J. Sandweiss, J. Sanford, H. Brown, M. Webster, and S. Yamamoto, Brookhaven National Laboratory Report No. BNL-6212, 1962 (unpublished).

[15] J. P. Berge, F. T. Solmitz, and H. D. Taft, Rev. Sci. Instr. **32**, 538 (1961).

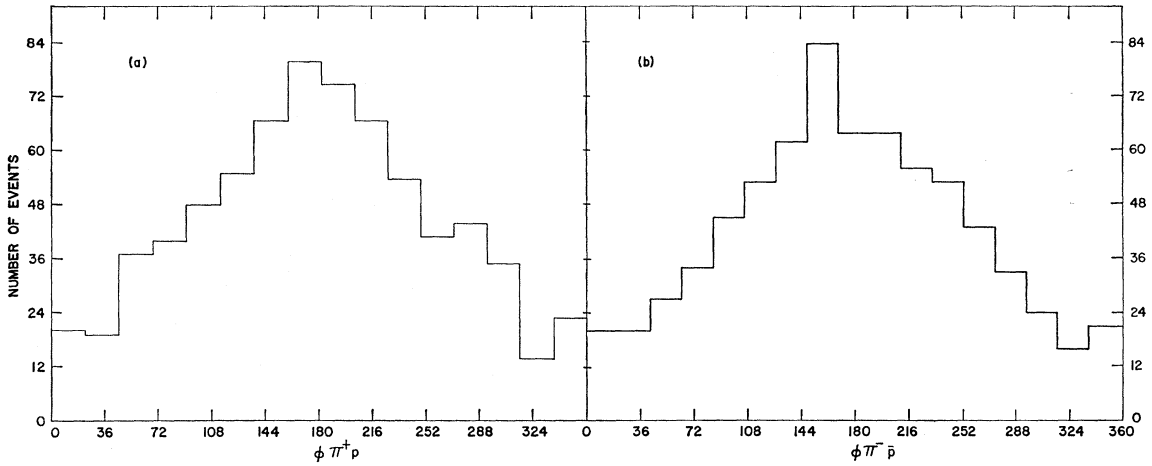

FIG. 1. (a) Distribution of the number of events with respect to the angle between the projections of the final π^+ and p momenta onto the plane normal to the incident $\bar{p}$ momentum (in the c.m. system). (b) The same distribution for the final π^- and $\bar{p}$.

to such tests. In particular, the following comparisons were made: (1) the effective mass of $(p\bar{p}\pi^+)$ and of $(p\bar{p}\pi^-)$, (2) the effective mass of $(p\pi^+\pi^-)$ and of $(\bar{p}\pi^+\pi^-)$, (3) the effective mass of $(p\pi^+)$ and of $(\bar{p}\pi^-)$, (4) the effective mass of $(\bar{p}\pi^+)$ and of $(p\pi^-)$, (5) the angular distributions and the momentum distributions of the π^+ and π^- in the center-of-mass system, and (6) the angular distributions and the momentum distributions of the p and $\bar{p}$ in the center-of-mass system. All of these comparisons were consistent with the requirements of the appropriate (C or CP invariance) test. In addition, the test suggested by Pais[16] is shown in Fig. 1. The distribution of the number of events with respect to the angle between the projections of the final π^+ and p

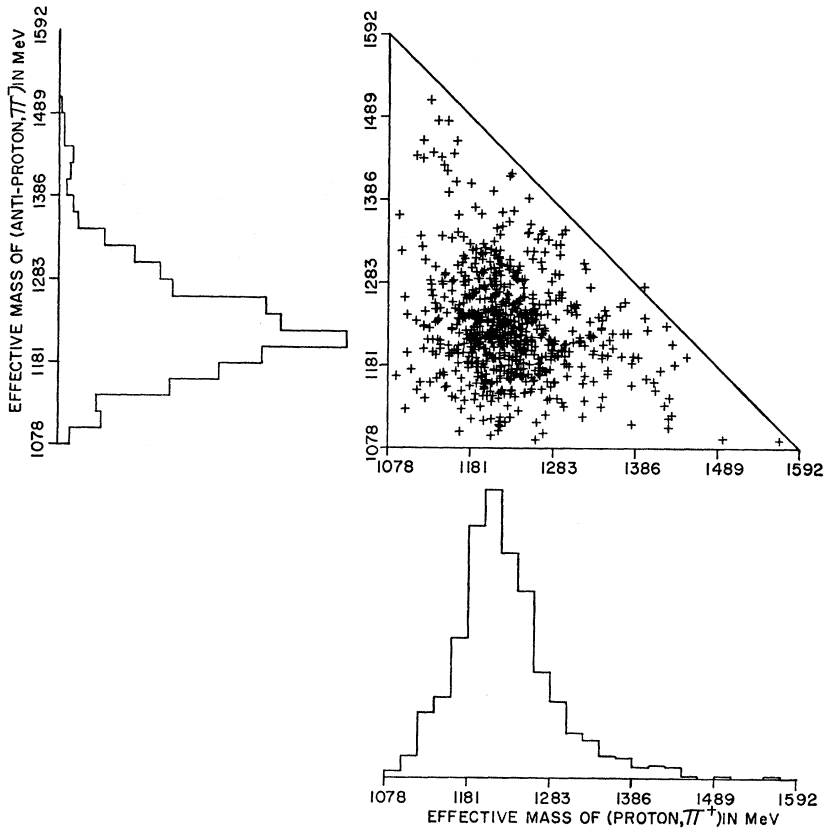

FIG. 2. Two-dimensional distribution of the effective masses of the final π^+p and $\pi^-\bar{p}$ combinations. The individual effective-mass distributions of the π^+p and $\pi^-\bar{p}$ systems are shown as projections. The figure is based on 719 events and each event occurs once.

[16] A. Pais, Phys. Rev. Letters 3, 242 (1959).

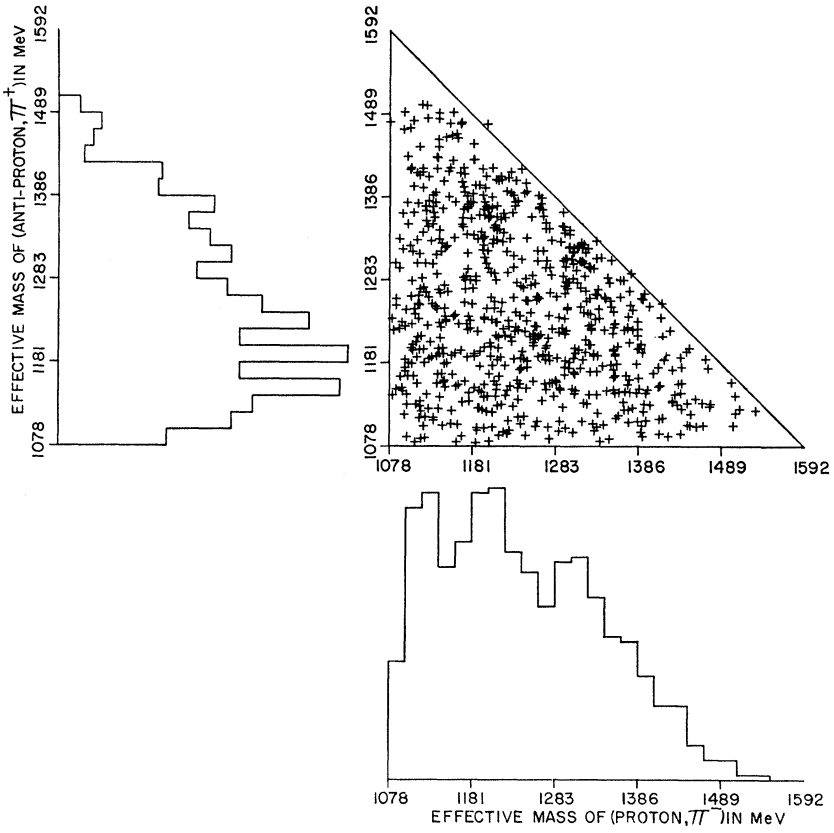

FIG. 3. Two-dimensional distribution of the effective masses of the final $\pi^+\bar{p}$ and π^-p combinations. The individual effective-mass distributions of the $\pi^+\bar{p}$ and π^-p systems are shown as projections. The figure is based on 719 events and each event occurs once.

momenta onto the plane normal to the incident $\bar{p}$ momentum (in the c.m. system) is shown in Fig. 1(a). The corresponding distribution for the final π^- and $\bar{p}$ is shown in Fig. 1(b). CP invariance requires the distributions to be identical, and the addition of C invariance further requires them to be symmetric about 180°. Within statistics these requirements are satisfied.

III. EXPERIMENTAL RESULTS

The total cross section for reaction (1) was found to be 1.93 ± 0.16 mb based on 719 events.

The reaction was found to proceed primarily through $N^*\bar{N}^*$ production, N^* being the $T=T_Z=J=\frac{3}{2}$ isobar of mass 1238 MeV. The dominance of double resonance production is seen in Fig. 2, a two-dimensional plot of the invariant mass of the outgoing π^+p and $\pi^-\bar{p}$ combinations. The theoretical expression for this invariant-mass distribution was written as

$$L(\omega,\tilde{\omega})=\alpha_{\pi^+p\pi^-\bar{p}}F_{\pi^+p\pi^-\bar{p}}+\alpha_{N^*\pi^-\bar{p}}F_{N^*\pi^-\bar{p}}+\alpha_{\pi^+p\bar{N}^*}F_{\pi^+p\bar{N}^*}+\alpha_{N^*\bar{N}^*}F_{N^*\bar{N}^*}. \quad (3)$$

In this expression, ω ($\tilde{\omega}$) is the effective mass of the outgoing π^+p ($\pi^-\bar{p}$) combination, the α's are the fractions of the events of the type indicated by the subscripts, and the F's are the corresponding invariant mass distributions (see Appendix). The result of a maximum-likelihood calculation using Eq. (3) is $\alpha_{\pi^+p\pi^-\bar{p}}=0.07\pm0.01$, $\alpha_{N^*\pi^-\bar{p}}=\alpha_{\pi^+p\bar{N}^*}=0.00\pm0.02$, $\alpha_{N^*\bar{N}^*}=0.93\pm0.01$. The errors quoted are purely statistical and do not reflect uncertainties in the forms used for the invariant-mass distributions in Eq. (3), i.e., in the F's. Small variations that were made in the forms of

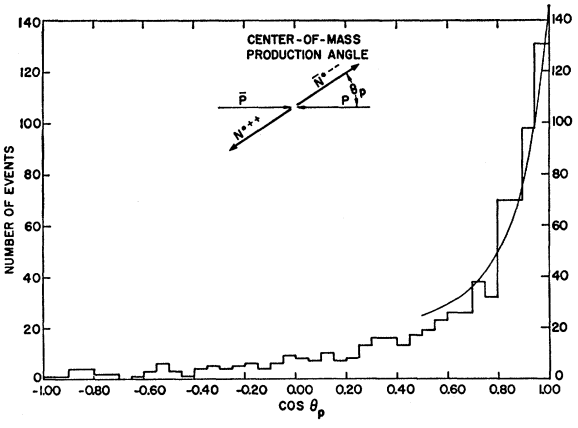

FIG. 4. Differential cross section with respect to the cosine of the angle between the incoming $\bar{p}$ momentum and the momentum of the outgoing $\pi^-\bar{p}$ system in the c.m. frame. The solid curve is the absorption-model prediction normalized to the number of events (533) in the region $0.5\leq\cos\theta_p\leq1.0$ (Ref. 23). The figure is based on 719 events.

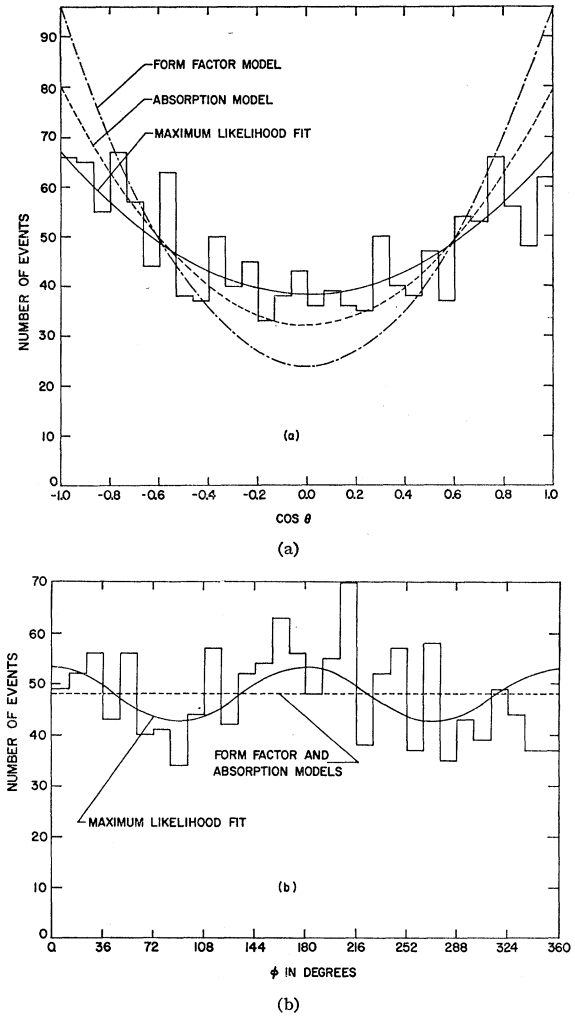

FIG. 5. (a) Distribution of the number of events with respect to the decay angle θ, defined as the angle between the incoming p ($\bar{p}$) and the outgoing π^+ (π^-) momenta in the rest frame of the outgoing π^+p ($\pi^-\bar{p}$) system. Since each event occurs twice, the histogram contains 1438 points. The solid curve is a plot of Eq. (5) using the density matrix elements obtained from a maximum-likelihood fit of Eq. (4) to the data. The other curves shown are the predictions of the form-factor and absorption models normalized to the data. (b) Distribution of the number of events with respect to the azimuthal decay angle φ. The solid curve is a plot of Eq. (6) using the density matrix elements obtained from a maximum-likelihood fit of Eq. (4) to the data. The dashed curve is the prediction of both the form-factor and absorption models normalized to the data.

the F's result in $0.90\leq\alpha_{N^*\bar{N}^*}\leq1.00$ and $0\leq\alpha_{\pi^+p\pi^-\bar{p}}+\alpha_{N^*\pi^-\bar{p}}+\alpha_{\pi^+p\bar{N}^*}\leq0.10$. On this evidence the best estimate for the fraction of double resonance production is $\alpha_{N^*\bar{N}^*}=0.95\pm0.05$. In the remainder of this paper this result is considered to be consistent with 100% double resonance production.

No N^* resonances with $T_Z=\frac{1}{2}$ were found. Figure 3, which is a plot of the π^-p and $\pi^+\bar{p}$ invariant masses, shows no enhancement near 1238 MeV. The $N^*(1518)$ is close to the kinematic limit and is not observed.

All other invariant-mass distributions were studied. No evidence of ρ production was seen in the $\pi^+\pi^-$ effective-mass distribution. The ρ mass lies very close to the kinematic limit of 790 MeV. In the $p\pi^+\pi^-$ and $\bar{p}\pi^+\pi^-$ mass distributions no enhancements were seen in the regions of the $N^*(1518)$ or $N^*(1688)$.

The distribution with respect to the cosine of the center-of-mass production angle is shown in Fig. 4. The production angle θ_p is defined as the angle between the incoming $\bar{p}$ momentum and the momentum of the outgoing $\pi^-\bar{p}$ system. Of the 719 events 50% occur with $\cos\theta_p>0.8$, i.e., the angular distribution of the $\bar{N}^*$ is strongly peaked in the forward direction.

The general form for the angular distribution of the N^* decay products (πN) in the N^* rest frame is[17]

$$W(\theta,\varphi)=C\{(\tfrac{1}{2}-\rho_{1,1})\sin^2\theta+\rho_{1,1}(\tfrac{1}{3}+\cos^2\theta)-(2/\sqrt{3})\,\mathrm{Re}\rho_{3,-1}\sin^2\theta\cos2\varphi-(2/\sqrt{3})\,\mathrm{Re}\rho_{3,1}\sin2\theta\cos\varphi\},\quad(4)$$

where θ is the angle between the incoming p ($\bar{p}$) and the outgoing π^+ (π^-) momenta in the N^* ($\bar{N}^*$) rest frame and φ is the corresponding azimuthal angle. The ρ's are density matrix elements and C is a normalization constant. The individual θ and φ distributions are obtained from (4) by integration over φ and θ, respectively:

$$W_1(\theta)=C_1\{(\tfrac{3}{4}-\rho_{1,1})+3(\rho_{1,1}-\tfrac{1}{4})\cos^2\theta\},\quad(5)$$

$$W_2(\varphi)=C_2\{1-(4/\sqrt{3})\,\mathrm{Re}\rho_{3,-1}\cos2\varphi\},\quad(6)$$

where, again, C_1 and C_2 are normalization constants.

The density matrix elements $\rho_{1,1}$, $\mathrm{Re}\rho_{3,-1}$, and $\mathrm{Re}\rho_{3,1}$ (averaged over the production angle) were determined by a maximum-likelihood calculation using Eq. (4) and the combined N^* and $\bar{N}^*$ decay data. The result is $\rho_{1,1}=0.350\pm0.015$, $\mathrm{Re}\rho_{3,-1}=-0.048\pm0.013$, and $\mathrm{Re}\rho_{3,1}=0.039\pm0.015$. Curves obtained using these values in Eqs. (5) and (6) are shown with the data in Fig. 5. The distribution of the azimuthal decay angle φ, Fig. 5(b), shows a definite departure from isotropy. The density matrix elements as functions of the cosine of the center-of-mass production angle were calculated using maximum-likelihood techniques and the results are shown in Fig. 6.

No correlation between the θ decay angle for the N^* and the θ decay angle for $\bar{N}^*$ was found.

IV. COMPARISON OF THE DATA WITH THE ONE-MESON-EXCHANGE MODELS

The data presented in Sec. III indicate the possibility of interpretation using one-pion-exchange models. Specifically, Fig. 4 shows a large peak in the number of events for small production angles, i.e., reaction (1) is highly "peripheral." In this section the data are com-

[17] K. Gottfried and J. D. Jackson, Nuovo Cimento 33, 309 (1964).

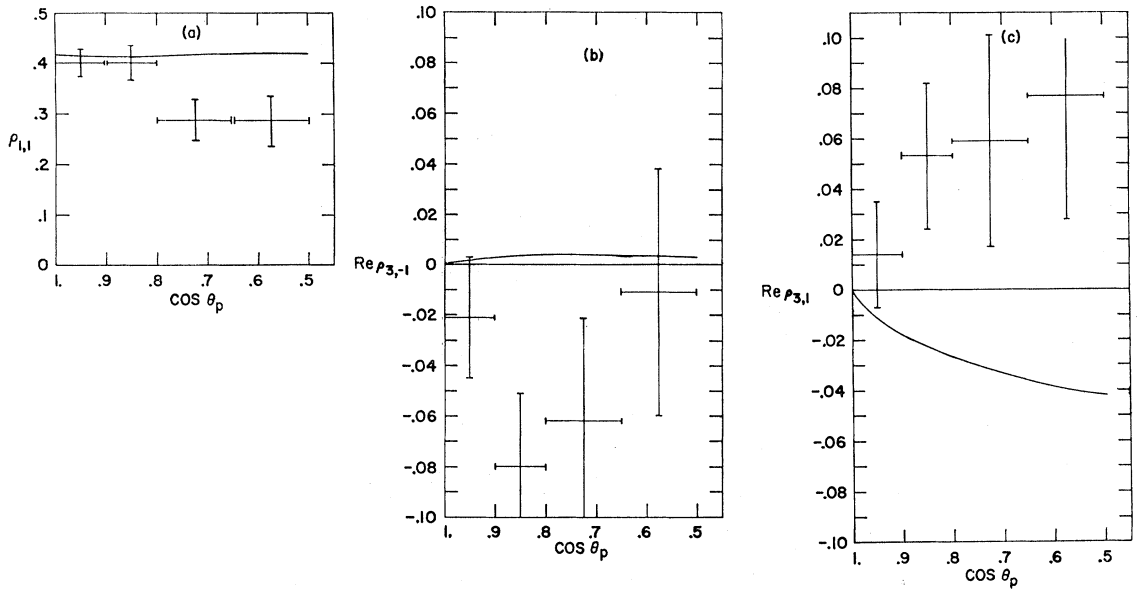

FIG. 6. Density matrix elements as a function of the cosine of the production angle θ_p. The solid curves are the predictions of the absorption model (Ref. 23).

pared with the predictions of the form-factor and absorption models.

The Form-Factor Model

In the present comparison of the predictions of the form-factor model with the data for reaction (1) only the contribution of the "double-isobar" diagram (Fig. 7) is included. The contribution of the $T_Z=\frac{1}{2}$ diagram (obtained by interchanging the outgoing π^+ and π^- of Fig. 7) was calculated to be approximately 1% of that of the double-isobar diagram and hence is neglected. The two "Drell" diagrams, in which a π^0 is exchanged producing both final pions at the same vertex, can contribute only to zero or single resonance production. Since the data presented in Sec. III are interpreted as 100% double-resonance production, the contribution of the Drell diagrams is neglected on empirical grounds. Further, possible contributions from ρ exchange are not included.

The differential cross section for reaction (1) given by the double-isobar diagram is[8]

$$\frac{d\sigma}{d\omega^2 d\bar{\omega}^2 d\Delta^2}=\Omega(\omega,\bar{\omega},\Delta^2)\frac{1}{16\pi^3 F^2}\times\bar{\omega}P(\bar{\omega};M^2,m^2)\sigma_1(\bar{\omega})\frac{1}{(\Delta^2+m^2)^2}\times\omega P(\omega;M^2,m^2)\sigma_1(\omega), \quad (7)$$

where M (m) is the nucleon (pion) mass, ω ($\bar{\omega}$) is the invariant mass of the final π^+p ($\pi^-\bar{p}$) system, Δ^2 is the square of the four-momentum transfer from the incoming $\bar{p}$ to the outgoing $\pi^-\bar{p}$ system, and F^2 is a kinematical factor defined by $F^2=(p_1\cdot p_2)^2-M^4$, where p_2 (p_1) is the incoming p ($\bar{p}$) four-momentum. $P(\omega;M^2,m^2)$ [$P(\bar{\omega};M^2,m^2)$] is the three-momentum of the final π^+ [π^-] in the final π^+p [$\pi^-\bar{p}$] c.m. system and is given by

$$P(\omega;M^2,m^2)=(2\omega)^{-1}\times[\omega^4-2\omega^2(M^2+m^2)+(M^2-m^2)^2]^{1/2}. \quad (8)$$

$\sigma_1(\omega)$ [$\sigma_1(\bar{\omega})$] is the total cross section for the $\pi^+p\to\pi^+p$ [$\pi^-\bar{p}\to\pi^-\bar{p}$] scattering process occurring at the lower [upper] vertex of the double-isobar diagram. For $\sigma_1(\omega)$ the Breit-Wigner form is used[18]:

$$\sigma_1(\omega)=\frac{2\pi}{[P(\omega;M^2,m^2)]^2}\times\frac{[\Gamma(\omega)]^2}{(\omega-\omega_0)^2+[\frac{1}{2}\Gamma(\omega)]^2}, \quad (9)$$

with the empirical resonance width expression

$$\Gamma(\omega)=2\gamma_\lambda^2[P(\omega;M^2,m^2)a]^3/[1+\{P(\omega;M^2,m^2)a\}^2],$$

where $2\gamma_\lambda^2=116$ MeV, $a=0.88m^{-1}$, $\omega_0=1237$ MeV, and $P(\omega;M^2,m^2)$ is defined in Eq. (8).

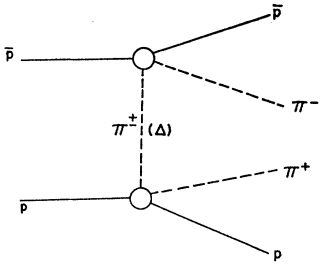

FIG. 7. "Double-isobar" one-pion-exchange diagram for the reaction $\bar{p}p\to\bar{p}p\pi^+\pi^-$.

[18] M. Gell-Mann and K. M. Watson, Ann. Rev. Nucl. Sci. 4, 219 (1954).

The factor Ω is a product of form factors and off-shell correction factors:

$$\Omega(\omega,\bar{\omega},\Delta^2) = [K'(\Delta^2)\cdot K(\Delta^2)R(\omega,\Delta^2)\cdot K(\Delta^2)R(\bar{\omega},\Delta^2)]^2. \quad (10)$$

$K'(\Delta^2)$ is the (unknown) form factor for the pion propagator, while $K(\Delta^2)R(\omega,\Delta^2)$ $[K(\Delta^2)R(\bar{\omega},\Delta^2)]$ corrects the total cross section $\sigma_1(\omega)$ $[\sigma_1(\bar{\omega})]$ for the fact that the exchanged pion is virtual. $K(\Delta^2)$ is the (unknown) form factor[19] for the pion-nucleon vertex and R is a known function obtained by Selleri.[20,21] The product of unknown form factors, K^2K', which occurs in Ω has been fitted to the $NN\to NN\pi$ data by Selleri[20] and is

$$K^2(\Delta^2)K'(\Delta^2)=8m^2/(\Delta^2+9m^2). \quad (11)$$

Thus Eq. (7) contains no undetermined parameters.

The predictions of the form-factor model for the present experiment are shown in Figs. 5, 8, and 9, where all theoretical curves are normalized to the data. The theoretical differential cross section with respect to the square of the four-momentum transfer from the initial $\bar{p}$ to the final $\pi^-\bar{p}$ system is compared with the data in Fig. 8. The theoretical curve is too sharply peaked and falls off too rapidly at higher momentum transfers, but as a whole is in fair agreement with the histogram. The shape of the theoretical curve would be somewhat improved by including the contribution from the Drell diagrams, but, as mentioned above, this is not consistent with the observed 100% double-isobar production. The invariant-mass distribution of the final π^+p and $\pi^-\bar{p}$ systems predicted by the form-factor model is compared with the data in Fig. 9. (The $\pi^-\bar{p}$ and π^+p invariant-mass histograms are combined.) The empirical Breit-Wigner resonance forms, Eq. (9), have a peak at 1225 MeV. The effect of the form factors and off-shell correction factors of Eq. (10) is to bring the peak of the predicted invariant-mass distribution down to 1218 MeV so that the theoretical curve is in good agreement with the data.

The form-factor model for reaction (1), as based on the double-isobar diagram, assumes the dominance of one diagram with the exchange of a spinless particle and no final-state interactions. Under these assumptions the density matrix elements of Eqs. (4), (5), and (6) are predicted to be[12] $\rho_{1,1}=\frac{1}{2}$, and $\rho_{3,1}=\rho_{3,-1}=0$, which may be compared with the experimentally determined values given in Sec. III. Thus the distribution $W_1(\theta)$ has the simple form $1+3\cos^2\theta$, while $W_2(\varphi)$ is independent of the azimuthal decay angle φ, i.e., the distribution in φ is predicted to be isotropic. (This result for W_1 and W_2 is, of course, the decay distribution observed for a "free" N^*.) In Fig. 5(a) the $1+3\cos^2\theta$ form for $W_1(\theta)$ (labeled form-factor model) is compared with the data. The agreement is seen to be poor. In Fig. 5(b) the theoretical distribution $W_2(\varphi)$, predicted isotropic in φ, is represented by a straight line. As pointed out in Sec. III the experimental distribution is not isotropic.

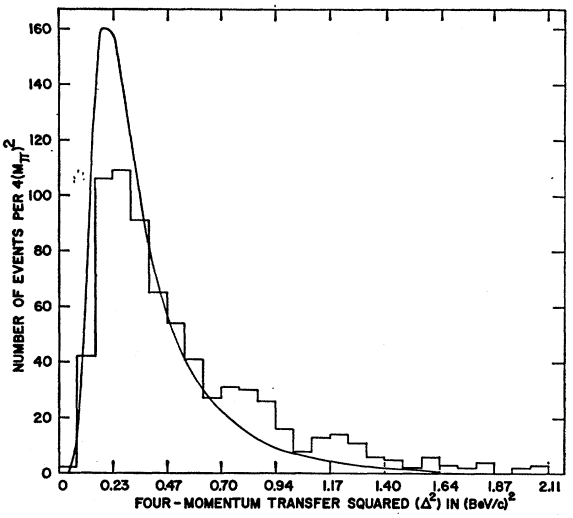

FIG. 8. Differential cross section with respect to the square of the four-momentum transfer from the incident $\bar{p}$ to the final $\pi^-\bar{p}$ system. The histogram is based on 719 events. The solid curve is the prediction of the form-factor model calculated from Eq. (7). The theoretical curve is normalized to the data.

The form-factor model based only on the double-isobar diagram[22] predicts a total cross section for reaction (1) at 2.7 BeV/c of 1.62 mb which is in good agreement with the experimental value of 1.93 ± 0.16 mb.

The Absorption Model

Hite and Jackson[23] have calculated the absorption-model predictions for the reaction $\bar{p}p\to\bar{N}^*N^*$. The essentials of their calculation are:

(a) An exact summation of the series of modified partial wave amplitudes is performed instead of approximating the sum by an integral over an impact parameter as is usually done.[12]

[19] K and K' are defined such that $K(-m^2)=K'(-m^2)=1$.

[20] F. Selleri, Nuovo Cimento **40**, 236 (1965). The authors are indebted to Professor Selleri for his results in advance of publication.

[21] The function $R(\omega,\Delta^2)$ is valid only in the "3,3 resonance region," but because of the low total c.m. energy in the present experiment the full range of $\omega(\bar{\omega})$ is included in this region.

[22] The theoretical contribution of the two Drell diagrams to the total cross section is $\sim$1 mb at 2.7 BeV/c. Thus the total cross section predicted by the form-factor model including *all* one-pion-exchange diagrams is 2.6 mb; in other words, the Drell diagrams would account for 40% of the predicted total cross section. The inclusion of the Drell diagrams in the predictions of the form-factor model would (1) reduce the sharpness of the peak of the predicted $d\sigma/d\Delta^2$ distribution and would make the distribution too large for $\Delta^2\gtrsim0.4$ (BeV/c)^2, and (2) completely destroy the agreement between the theoretical curve and the histogram for the invariant $\pi^+p(\pi^-\bar{p})$ mass distribution.

[23] G. E. Hite and J. D. Jackson (private communication). Dr. Hite and Professor Jackson have kindly supplied the authors with the details of their calculation and with the theoretical absorption-model curves shown in Figs. 4, 6, and 9.

(b) The absorption parameters in the initial ($\bar{p}p$) and final ($\bar{N}^*N^*$) states are $\gamma_1=0.03$, $C_1=1.0$, and $\gamma_2=0.01$, $C_2=1.0$, respectively (in the notation of Ref. 12). These absorption parameters are chosen, within the freedom allowed by the errors in the $\bar{p}p$ elastic-scattering data, to improve the predictions of the absorption model for the present experiment, particularly to improve the fit to the differential cross section $d\sigma/d(\cos\theta_p)$ and to the total cross section.

(c) The $N^*N\pi$ coupling constant used is $G^{*2}/4\pi=0.428$ (in the notation of Ref. 24).

(d) The calculated differential cross section for the production of the two "stable" isobars is multiplied by two Breit-Wigner resonance expressions to include the effects of the resonance decays. The resonance expressions are of the type discussed by Jackson[25] with the usual P-wave resonance width modified to include about 10% S wave. The value of ω_0 was chosen as 1230 MeV instead of the usual 1237 MeV. These two modifications are made to improve the absorption-model prediction of the invariant-mass distribution for the present experiment.

The predictions of the absorption-model calculation of Hite and Jackson are shown in Figs. 4, 5, 6, and 9, where the theoretical curves are normalized to the data. The theoretical curve and the histogram for the differential cross section with respect to the production angle are shown in Fig. 4. The agreement is good, but the theoretical curve is not peaked as strongly at small angles as the data. The theoretical curve and the data for the invariant-mass distribution of the final isobars are shown in Fig. 9. The agreement is good.

Although the absorption-model calculation for $\bar{p}p\rightarrow\bar{N}^*N^*$ involves the dominance of a single diagram with the exchange of a spinless particle, the inclusion of initial- and final-state interactions means that the density matrix elements predicted by the absorption model will differ from those predicted by the form-factor model. The theoretical and experimental density matrix elements as a function of the production angle are shown in Fig. 6. The theoretical and experimental values of

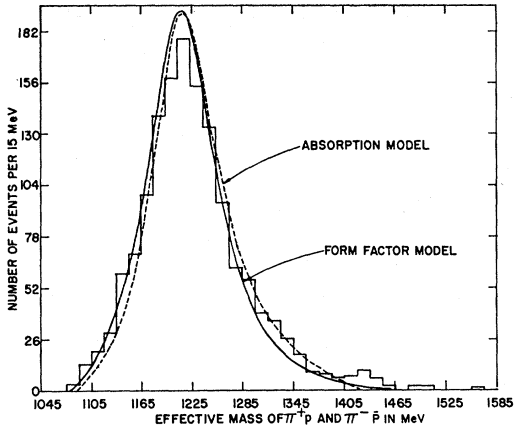

FIG. 9. Distribution of the number of events with respect to the π^+p and $\pi^-\bar{p}$ effective masses (1438 data points). The solid curve is the prediction of the form-factor model calculated from Eq. (7). The dashed curve is the prediction of the absorption model (Ref. 23). Both theoretical curves are normalized to the data.

$\rho_{1,1}$ agree at small production angles, but diverge with increasing production angle. For $\mathrm{Re}\rho_{3,-1}$ and $\mathrm{Re}\rho_{3,1}$ the theoretical predictions are inconsistent with the data. The absorption-model prediction for the decay distribution $W_1(\theta)$ is shown with the data in Fig. 5(a). The agreement is adequate. The theoretical decay distribution $W_2(\varphi)$ predicted by the absorption model is shown as a straight line in Fig. 5(b) because the predicted value of $\mathrm{Re}\rho_{3,-1}$ is too small to produce a detectable deviation from isotropy. As remarked in Sec. III the observed distribution is not isotropic.

The absorption model predicts a total cross section of 2.2 mb for $\cos\theta_p\geq 0.5$. This is to be compared with an experimental cross section of 1.4 mb for events with this restriction.

V. CONCLUSIONS

The reaction $\bar{p}p\rightarrow\bar{p}p\pi^+\pi^-$ has been studied over a wide range of incident $\bar{p}$ momenta. The total cross section at six energies is given in Table I. The cross section rises slowly from the double-pion-production

TABLE I. Total cross sections for the reaction $\bar{p}p\rightarrow\bar{p}p\pi^+\pi^-$.

Incident $\bar{p}$ lab momentum (BeV/c)	Total cross section $\bar{p}p\rightarrow\bar{p}p\pi^+\pi^-$ (mb)	Fraction of $N^*(1238)$ production (%) zero ($p\pi^+\bar{p}\pi^-$)	single ($p\pi^+\bar{N}^*$ and $N^*\bar{p}\pi^-$)	double ($N^*\bar{N}^*$)	Reference
2.7	1.93±0.16	0	0	100	present paper
3.28	3.43±0.23	···	···	80	1
3.6	3.80±0.22	···	···	56	2
3.66	3.67±0.30	···	···	50–80[a]	1
5.7	3.18±0.16	20	50	30	3
5.7	3.31±0.16	16	21	63	4
6.94	3.0 ±0.7	···	···	50	5

[a] The 50% figure is obtained from a comparison of the form-factor model (including Drell diagrams) with the data. The 80% figure is obtained by fitting the invariant $\pi^+p(\pi^-p)$ mass distribution with phase space and S-wave Breit-Wigner shapes with peaks at 1215 MeV and $\Gamma=90$ MeV.

[24] J. D. Jackson and H. Pilkuhn, Nuovo Cimento 33, 906 (1964).
[25] J. D. Jackson, Nuovo Cimento 34, 1644 (1964).

threshold of 1.2 BeV/c, but rapidly from the double $N^*(1238)$ threshold of 2.0 BeV/c, remaining relatively constant for higher beam momenta. These facts reflect the importance of N^* formation in reaction (1). Also shown in Table I are estimates of the amounts of zero, single, and double resonance production. Near threshold reaction (1) appears to be dominated by double N^* formation, while substantial fractions of single and zero resonance production occur at higher energies.

The second outstanding characteristic of the data at all energies is that the differential cross section with respect to the square of the four-momentum transfer from the initial $\bar{p}$ to the final $\pi^-\bar{p}$ system ($d\sigma/d\Delta^2$) is sharply peaked at small Δ^2. The shape of the peak does not change appreciably with energy, however larger fractions of events with high four-momentum transfer occur as the energy is increased.

In the present paper the density matrix elements are given as a function of production angle at 2.7 BeV/c. Svensson[26] gives the density matrix elements as a function of the square of the four-momentum transfer at 3.6 and 5.7 BeV/c. A comparison of Fig. 6 and Svensson's results shows that $\rho_{1,1}$ does not vary in magnitude or in Δ^2 dependence as the incident $\bar{p}$ momentum is changed. This means that the cosθ decay distribution does not change appreciably with energy. In contrast to this, the values of Re$\rho_{3,-1}$ and Re$\rho_{3,1}$ vary considerably with energy. At 2.7 BeV/c the value of Re$\rho_{3,-1}$ is four standard deviations from zero, and the φ decay distribution is anisotropic. At higher energies the decay distribution is observed to be isotropic, and the values of Re$\rho_{3,-1}$ are consistent with zero. The density matrix element Re$\rho_{3,1}$ has small positive values at 2.7 BeV/c, values consistent with zero at 3.6 BeV/c, and small negative values at 5.7 BeV/c. No correlation between the θ decay angles for the N^* and the $\bar{N}^*$ is observed at 2.7 BeV/c, while a small correlation is observed at higher beam momenta.

ACKNOWLEDGMENTS

The authors would like to express their gratitude to the operating staff of the AGS and of the 20-in. bubble chamber and also to Dr. H. Brown and Dr. J. Sanford. We are indebted to the scanning, measuring, and programming staffs of Iowa State University, in particular to W. Higby, B. Pepper, and R. Wagstaff. We are grateful for conversations with Professor R. H. Good and for correspondence with Professor T. A. Ferbel and Professor F. Selleri. We are indebted to Professor J. D. Jackson and Dr. G. E. Hite for supplying us with the results of their calculations and for helpful conversations.

[26] B. E. Y. Svensson, Nuovo Cimento **39**, 667 (1965). This paper contains the predictions of the absorption model for reaction (1) at 3.6 and 5.7 BeV/c.

APPENDIX

The two-dimensional invariant-mass distribution as given by Eq. (3) contains phenomenological forms for zero resonance production ($F_{\pi^+p\pi^-\bar{p}}$, four-body phase space), for single resonance production ($F_{N^*\pi^-\bar{p}}$ and $F_{\pi^+p\bar{N}^*}$), and for double resonance production ($F_{N^*\bar{N}^*}$) which are products of phase-space factors and Breit-Wigner resonance expressions. These F's are[25]

$$F_{\pi^+p\pi^-\bar{p}}=C_1\frac{P(\omega;M^2,m^2)}{\omega}\frac{P(\tilde{\omega};M^2,m^2)}{\tilde{\omega}}\frac{P(E;\omega^2,\tilde{\omega}^2)\omega\tilde{\omega}}{E},$$

$$F_{N^*\pi^-\bar{p}}=C_2F_{\pi^+p\pi^-\bar{p}}\varphi(\omega),$$

$$F_{\pi^+p\bar{N}^*}=C_3F_{\pi^+p\pi^-\bar{p}}\varphi(\tilde{\omega}),$$

$$F_{N^*\bar{N}^*}=C_4F_{\pi^+p\pi^-\bar{p}}\varphi(\omega)\varphi(\tilde{\omega}),$$

where the C's are normalization constants, ω ($\tilde{\omega}$) is the effective mass of the final π^+p ($\pi^-\bar{p}$) combination, M (m) is the nucleon (pion) mass, and E is the total energy in the over-all c.m. system. $P(\omega;M^2,m^2)$ is the magnitude of the final π^+ three-momentum in the final π^+p rest frame:

$$P(\omega;M^2,m^2)=(2\omega)^{-1}[\omega^4-2\omega^2(M^2+m^2)+(M^2-m^2)^2]^{1/2}.$$

$\varphi(\omega)$ is defined by

$$\varphi(\omega)=\frac{\omega}{P(\omega;M^2,m^2)}\frac{\Gamma(\omega)}{(\omega^2-\omega_0^2)^2+\omega_0^2\Gamma^2(\omega)},$$

where

$$\Gamma(\omega)=\Gamma_0\left\{\frac{P(\omega;\ M^2,m^2)}{P(\omega_0;M^2,m^2)}\right\}^3\left[\frac{2.2m^2+\{P(\omega_0;M^2,m^2)\}^2}{2.2m^2+\{P(\omega;\ M^2,m^2)\}^2}\right].$$

The quantity in square brackets is an empirical correction to the P-wave resonance width. ω_0 is the central value of the mass of the resonance and Γ_0 is the width parameter.

In the maximum-likelihood calculation the α's were subject to the restrictions

$$\alpha_{\pi^+p\pi^-\bar{p}}+\alpha_{N^*\pi^-\bar{p}}+\alpha_{\pi^+p\bar{N}^*}+\alpha_{N^*\bar{N}^*}=1,$$

$$\alpha_{N^*\pi^-\bar{p}}=\alpha_{\pi^+p\bar{N}^*}.$$

In addition to the α's, ω_0 and Γ_0 were also allowed to vary.